World Electric Vehicle Journal

MDPI

Article

Applications of Battery Management System (BMS) in Sustainable Transportation: A Comprehensive Approach from Battery Modeling to Battery Integration to the Power Grid

Sagar B S [1,*], Santoshkumar Hampannavar [1], Deepa B [2] and Bansilal Bairwa [1]

[1] School of Electrical and Electronics Engineering, REVA University, Bengaluru 560024, India; santoshkumar.sh@ieee.org (S.H.); bansilal.bairwa@reva.edu.in (B.B.)
[2] Rao Bahadur Y. Mahabaleswarappa Engineering College (RYMEC), Bellary 583275, India; deep.vc004@gmail.com
* Correspondence: sagar.bs14@gmail.com

Abstract: The growing oil demand and serious environmental concerns have promoted the concept of the usage of electric vehicles (EVs) across the globe. EVs can be integrated into the grid for power transaction and to support the grid requirements, thereby drawing the attention of researchers, policy makers and industries. EVs are not only a transportation tool but also act as a distributed source or load. The EV battery plays a prominent role in grid integration and sustainable transportation. The monitoring and control aspect of the battery management system (BMS) plays a vital role in the successful deployment and usage of EVs. In this paper, an equivalent circuit model (ECM) of battery is proposed and analyzed that describes the battery behavior at various temperatures, considering the internal resistance of the battery. A stochastic model was developed for the battery ageing and replacement to ensure that systematic replacement of batteries based on the calendar ageing was performed. A reliability assessment of EV accessibility and availability was carried out by using Markov chain. A case study of a Diesel-renewable powered Electric Vehicle Charging Station (EVCS) in a micro-grid was carried out that suits the requirement of large-scale EV fleet integration to the grid for power transaction. The holistic approach of BMS was considered for the sustainable transportation and grid integration

Keywords: electric vehicle; battery management system; equivalent circuit model; battery ageing; stochastic model; reliability

Citation: B S, S.; Hampannavar, S.; B, D.; Bairwa, B. Applications of Battery Management System (BMS) in Sustainable Transportation: A Comprehensive Approach from Battery Modeling to Battery Integration to the Power Grid. *World Electr. Veh. J.* **2022**, *13*, 80. https://doi.org/10.3390/wevj13050080

Academic Editor: Joeri Van Mierlo

Received: 12 March 2022
Accepted: 20 April 2022
Published: 6 May 2022

1. Introduction

The global transportation sector is looking toward cleaner means of mobility and electric vehicle support in this aspect. Cleaner transportation accounts for the use of battery-powered vehicles, often termed as electric vehicles (EVs). Batteries are the heart of the system that powers these vehicles. The advancement in battery technology drives the development of EVs. Almost all automakers have launched EVs, and the sales have been increasing steadily over the last decade. However, in order to popularize EVs as compared to internal combustion engines, EVs have to overcome many barriers, particularly in battery technology. The development of the battery management system (BMS) has made a significant contribution in the development of EVs. The BMS looks after all the criteria of batteries, including the charging and discharging process and battery life estimation and performance prediction. In this regard, various aspects of the battery are to be considered right from battery modeling to its reliability assessment. Battery parameters, such as its internal resistance, its capacity to hold the charge and time duration of its discharge, vary with aspects such as time, number of charge and discharge cycles, depth of discharge and temperature of operation. In this regard, batteries are to be carefully understood, especially during its lifetime. Battery modeling is a crucial aspect in understanding the

behavior of the battery. The lifetime of the battery is dependent upon its physical and chemical characteristics [1]. Battery modeling has its significance in developing efficient charging and discharging schemes thereby protecting the battery from overcharging and undercharging conditions. Finding the safe operating limits enhances the lifetime of the battery. Different modeling schemes are developed in the literature with different complexities suitable for different applications [2–4]. Electro-chemical models consisting of complex differential equations have been developed. Solving the equations provides details of battery parameters. The computation complexity is the major aspect in employing these models [5,6]. Analytical models have been developed over the years that model only the major properties of the batteries, often neglecting important parameters, such as internal resistance of the battery, thereby reducing the complexity. Peukert's law and Rakmatov and Vardhula are notable model analytical battery models [7]. Stochastic models have also been developed that have defined discharging and recovery effects as stochastic processes. As these models consider only relative number of lifetimes, it is unclear if they perform quantitatively [8–11]. A detailed review on modeling techniques and parameter extraction is presented in Reference [12]. However, there is a need to find an easy and efficient model to understand the behavior of the battery, and that model should also be validated by using experimental data. Electric circuit models were proposed which include a capacitor, representing the capacity of the battery; the discharge rate, which determines the lost capacity; a circuit to discharge the battery; a lookup table consisting of voltage versus state of charge (SOC); and a resistor, representing internal resistance of the battery. With minor modifications suitable to the application and chemistry of the battery, the models are reliable and accurate. In this study, a 3 R-C model was developed and validated to determine the behavior of the battery. The understanding of battery ageing is of paramount importance, as it has a direct impact on the performance of the battery. Diagnosing the battery age and acting on it not only ensures the safety of the battery-powered system but also enhances the lifetime and profitability of EVs [13–15]. In the literature, calendar ageing is often neglected, and random policies are employed to replace the batteries. However, replacing the batteries happens in a structured scheme [16]. The Markov chain-based battery ageing model is proposed, keeping in view the replacement of worn-out batteries which would be due for their replacement much earlier than the specified time of replacement. On the other side, the successful deployment of electric vehicles is possible only when they are reliable, safe and easy to maintain, as compared to the much popular and vastly deployed internal combustion engine [17,18]. The work concentrates on a mathematical model of EVs' reliability aspect and maintainability aspect and its analysis of all significant electrical and electronic components of EVs.

Section 2 deals with battery modeling, while Section 3 deals with a battery ageing and replacement model. The electric vehicle's architecture is framed, modeled for its operating and fault conditions; the reliability and maintainability aspects are developed and analyzed in Section 5. The results are discussed in Section 6. The significant contributions of this paper are as follows:

(i) Analysis of battery equivalent circuit model is carried out and substantiates that the 3 R-C model provides the best behavior of battery subjected to variations in temperature;
(ii) Development of stochastic model of battery ageing and replacement scheme, providing a systematic approach for replacing the aged batteries and, thus, avoiding system failure and exorbitant investment in replacing the battery pack at once;
(iii) Reliability assessment of electric vehicle is carried out which states that, with the required maintainability aspect, the life of the electric vehicle can be extended;
(iv) Diesel-renewable-based electric vehicle charging system assessment is carried out for techno-economic and environmental issues on raising carbon emissions.

2. Battery Modeling

Battery modeling is significant, as it is the key factor in developing improved charging and discharging schemes. This also helps in preventing the battery from overcharging

and undercharging, thereby preventing potential damage to the batteries. Overall, battery modeling provides operating limits that guide the best usage of batteries. Amongst different types of battery models, the equivalent circuit model is the most suitable to represent the features of the battery [19,20]. The run-time-based equivalent circuit model pairs electrical network with lookup tables to determine the parameters of the battery. Thevenin's models provide models based on R-C networks, which give steady-state and transient behavior to the battery. Circuit parameters are also obtained by an approach that compares the battery model simulation to the actual battery response. The work proposes the lithium-ion battery model under dynamic loading conditions, as per defined standard drive cycles. The literature proposes equivalent circuit models with n number of R-C branches to represent the behavior of the battery. However, the complexity and computational ability of the circuit increases with the increase in the number of R-C components. The work proposes that the 3 R-C model is best suited to represent the behavior of the battery based on experimental validation.

An equivalent circuit model was developed to estimate the behavior of the lithium battery. The model selected for the work is INR18650-20R. This model was further validated by using the dynamic current profile test, which has the advantage of regenerative breaking. An equivalent circuit model consists of an ideal voltage source, the R-C network, which represents the characteristics of the cell, including the internal resistance that plays a major role in defining the cell behavior. Each element of the circuit is a function of SOC and temperature. In Figure 1a–e, 1 R-C to 5 R-C models are represented.

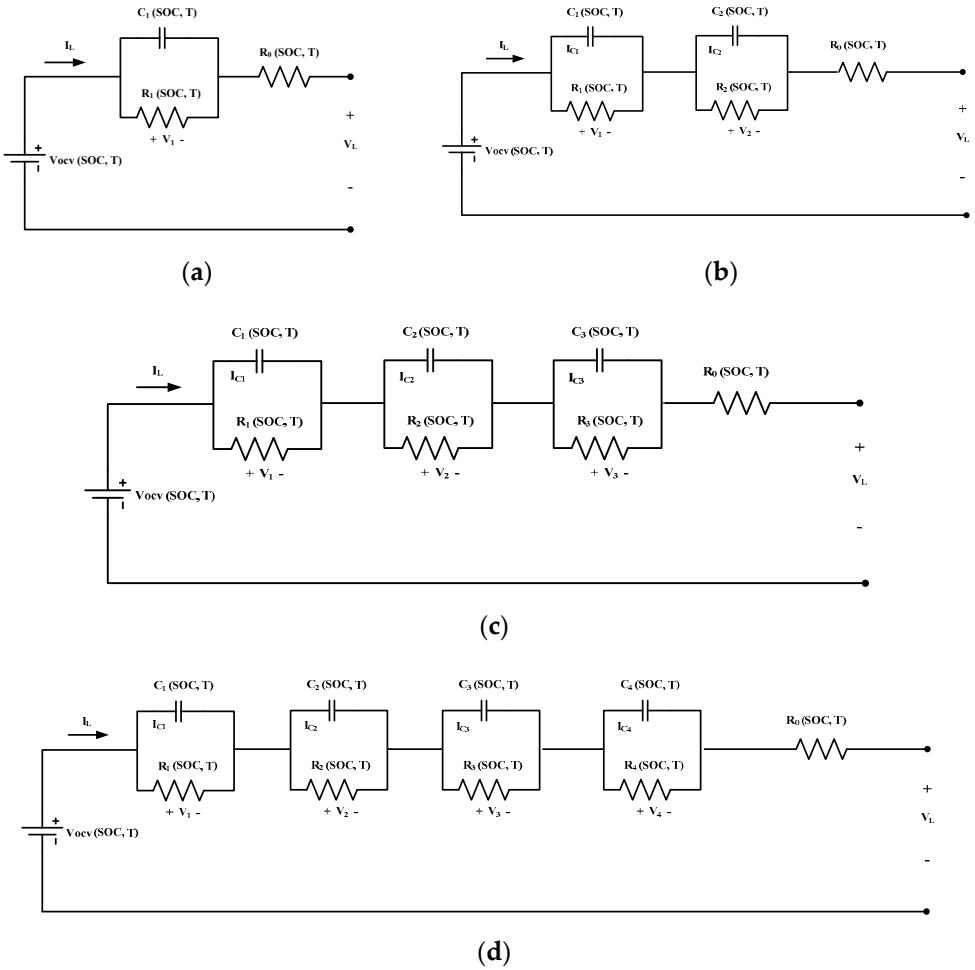

Figure 1. *Cont.*

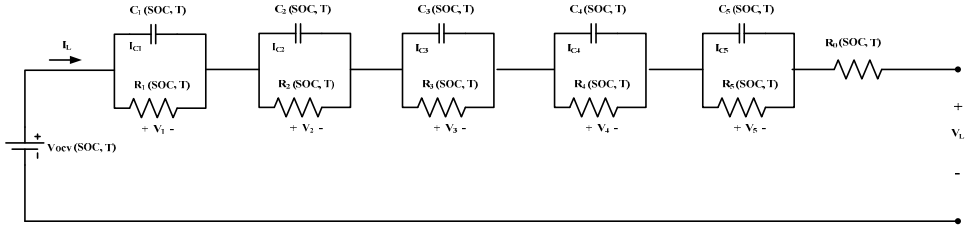

(**e**)

Figure 1. Equivalent circuit model of battery.

The voltage equation, V_L, is given by Equation (1). An Incremental Open Circuit Voltage (OCV) test at different temperatures is employed to estimate the parameters, using the developed models, which are given in Figure 2.

$$V_L = V_{OCV} - \left(\int_0^t \frac{I_L}{C_1} - \frac{V_1}{R_1C_1}\right) - \left(\int_0^t \frac{I_L}{C_2} - \frac{V_2}{R_2C_2}\right) - \left(\int_0^t \frac{I_L}{C_3} - \frac{V_3}{R_3C_3}\right) - \left(\int_0^t \frac{I_L}{C_4} - \frac{V_4}{R_4C_4}\right) - \left(\int_0^t \frac{I_L}{C_5} - \frac{V_5}{R_5C_5}\right) - I_L R_0 \quad (1)$$

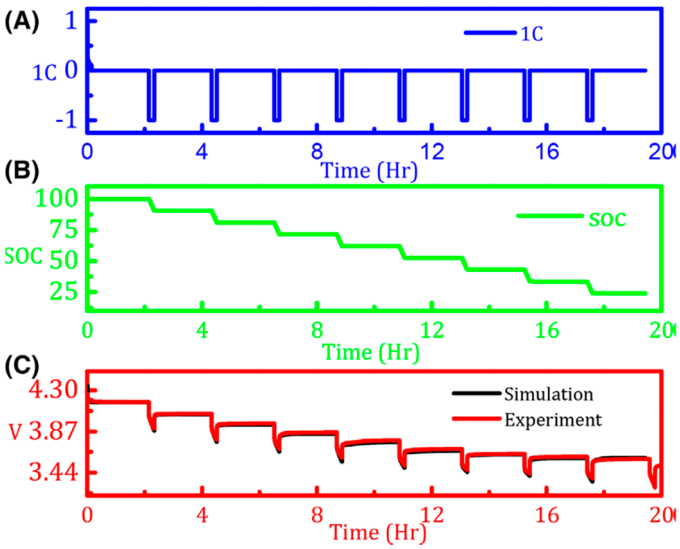

Figure 2. (**A**) Incremental Open Circuit Voltage load profile. (**B**) SOC under parameter estimation. (**C**) Simulated and experimental voltage response.

3. Stochastic Model of Battery Ageing and Replacement

Problems associated with the battery can be categorized into two groups, as shown in Figure 3. The energy demand for higher energy densities, especially in lithium-based batteries, is increasing. Various chemistries are proposed in meeting the higher power levels, but these advantages come with the caveat of having considerable change in volumes of silicon particles during lithiation and de-lithiation, causing the instability of the solid electrolyte interphase (SEI) formed on electrodes [21–23]. Battery degradation refers mainly to the loss of the charge-holding capacity of the battery and increase in its internal resistance. Degradation prediction can be well classified into two groups: based on calendar ageing and based on charge–discharge cycles. The paper is based on the former concept.

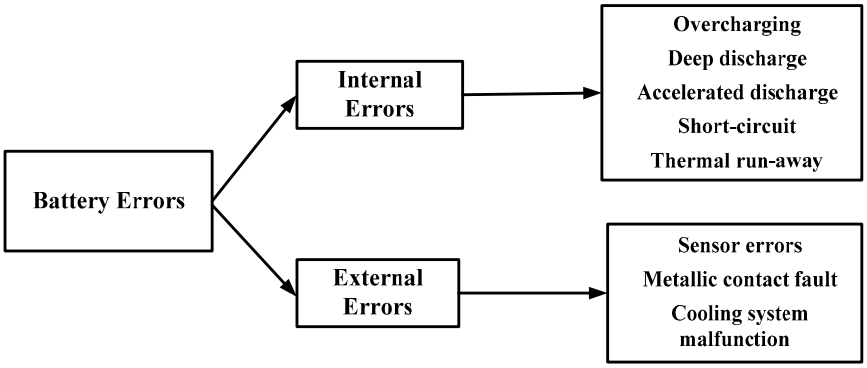

Figure 3. Battery errors.

As the batteries contribute significantly to the cost of the EV, the manufacturers are compelled to ensure that the battery life is maximized, so as to reduce the operational cost and replacement cost. As a result, identifying aging and malfunctioning batteries and developing analytical models for their replacement is important [24]. Leading battery manufacturers devise policies to replace the battery based on calendar ageing, while the industries will set its own timelines to replace the batteries. In the case of electric vehicles, the possible replacement will be set by the manufacturer. Some of the policies are mentioned in References [25–27].

Considering the inherent irregularities associated with the battery, the replacement process has to be carefully designed so as to replace only those batteries that are underperforming, while retaining the other batteries, thus avoiding one-shot exorbitant reinvestment at the end of the specified time period. As per the Per Green Car Reports, 2011–2014 model Nissan make Leafs having 24 kWh battery pack costs 5500 USD for replacement, while 2017 make Chevrolet Bolt having 60 kWh battery pack costs around 15,000 USD for replacement [28,29]. This exorbitant one-shot battery replacement cost can be avoided by predicting the battery behavior and replacing only that malfunctioning battery. The prediction of the battery life and its longevity is essential for any system dependent on the battery bank. The prediction and assessment are challenging tasks, as they require a complex and expensive experimental setup and rigorous calculations. The development of degradation models helps in predicting the degradation of the battery. The literature provides several ageing models. However, most of the models consume high amounts of data and involve a high number of iterations to compute the result. Some of the models require rigorous training [30–32].

In the literature, calendar ageing models for Li-ion batteries using transfer learning methods were discussed and presented. Characterization test data of the battery, storage temperature, SOC and estimated previous time step were fed as input to the neural network, resulting in the lost capacity of the battery. Due to the overfit, the model prediction was found to be poor.

3.1. Importance of Battery Calendar Ageing

The development of the Solid Electrolyte Interface (SEI) on the negative electrode is the major contributor for calendar ageing. Cycling ageing is mainly due to lithium plating of the negative electrode. As EVs spend most of the time at rest having lower current levels around 3C [33], calendar ageing of the battery also becomes a vital factor in the development of the battery ageing and replacement model. SEI formation on the negative electrode results in the consumption of cyclable lithium content, leading to an increase in the value of electrode impedance. In the acceleration stage, capacity fade is faster, due to SEI formation on the anode surface. With the increase in SEI interface, there is an isolation effect on the electrode, thus resulting in decrement in chemical reaction rate. This results in the stabilization mode of the battery, as shown in Figure 4. At this stage, the battery performance gradually drops down and eventually leads to early cutoff voltage for the

battery. In the saturation stage, the poor capacity on the cathode makes the cathode quickly saturate during discharge, and also quickly deplete during charge. The capacity fade in the discharged curves of an aged battery is shown in Figure 5, which indicates a high rate of capacity fade in the initial cycles, due to SEI. Moreover, the cycling aging affects the concentration and volume of the battery. The battery aging is path-dependent, especially when the battery is subjected to power cycles and calendar periods [33].

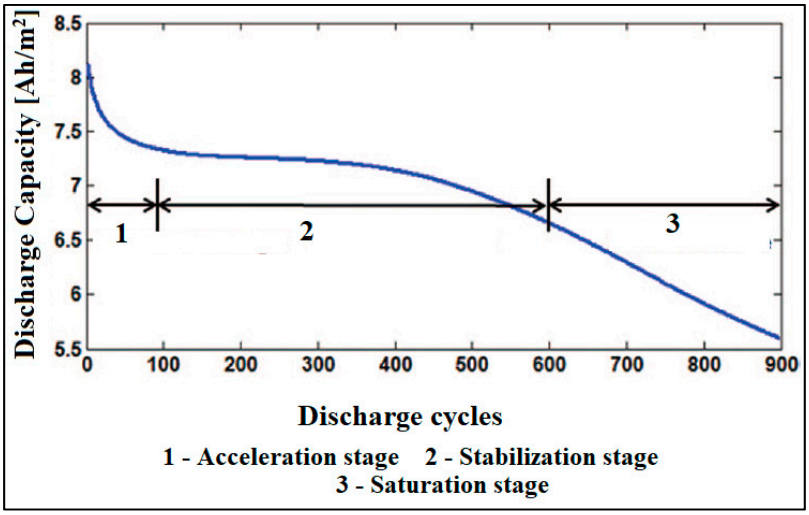

Figure 4. Decrement in chemical reaction rate.

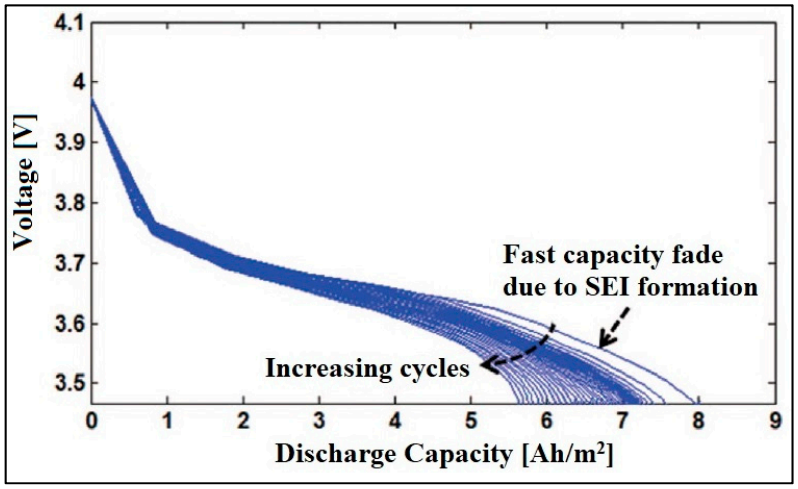

Figure 5. Capacity fade in aged battery.

3.2. Markov Model for Battery Ageing and Replacement

As Markov models are being used to characterize the EV behaviors in various mobility scenarios, we provide Markov chain analysis where it can be integrated with a battery management system. Considering the activity of EVs, the operation of EV can be categorized into three main cases, namely EVs at rest, EVs in drive mode and EVs in charge period only. These models are represented by Figures 6–8 respectively.

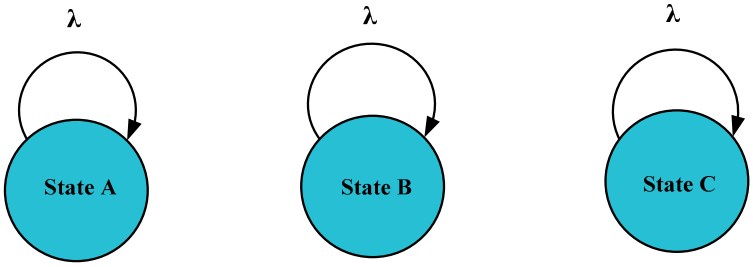

Figure 6. Battery model for EVs at rest, where State A corresponds to 100% SOC, State B corresponds to 50% SOC and State C corresponds to 0% SOC.

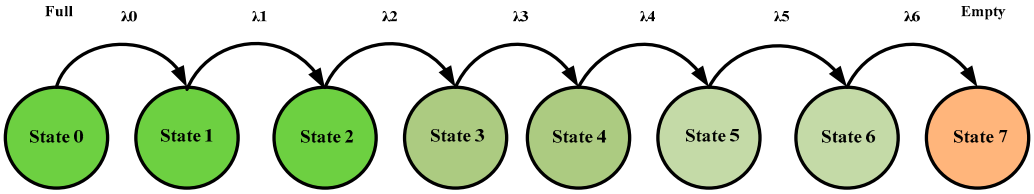

Figure 7. Battery discharge model.

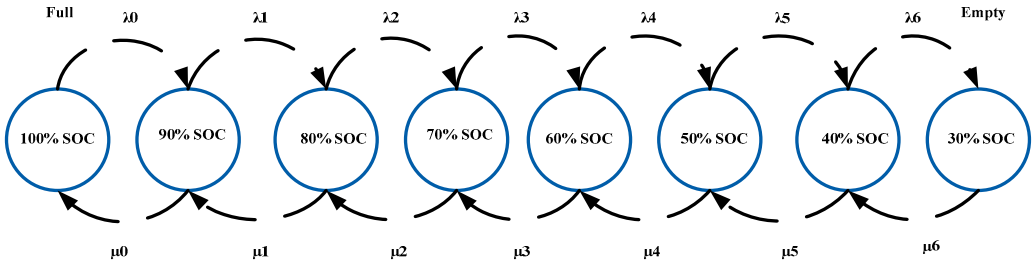

Figure 8. Battery charge–discharge model.

In the first case where EVs are at rest, the EVs are parked and are not connected to any charger. This condition provides only one scenario where the battery remains in its present state. Referring to the model below, if the battery is in State A (e.g., State A corresponding to 100% SOC), it remains in the same state. Similarly, the battery can be any state represented as State B (e.g., State B corresponding to 50% SOC) and State C (e.g., State C corresponding to 20% SOC). Also, when the battery is in this state, it is possible to analyze the effect of charge leakage, self-discharge and other effects inside the battery. However, considering the effect of charge and discharge on the battery, the effect of the above said parameters could be neglected.

The second case is where EVs' mode can be further subdivided into two categories, namely (i) EVs in the discharge cycle and (ii) EVs in discharge-and-charge cycle. EVs in the discharge cycle are EVs that are in use, with the batteries being drained continuously to power the vehicle. It is inherent that the battery is discharged in this mode. The EV can be assumed to return back to its own charging station (starting point of the drive cycle or pavilion) or any intermittent station after it reaches the predefined depleted state which corresponds to the point where the EV must be charged. The model can be represented by n states. However, the model represented consists of eight states, beginning from 100% SOC of the battery, represented by State 0, down to 30% SOC, represented by State 7, which is assumed to be the depleted state.

The probability matrix 'm' of the battery discharge model is represented in (2). The probability with which there is change in the states is represented by λ_n, where n is from 0

to 6, representing transition numbers. Various state equations are represented in Equations (3) and (4), where $S1$ represents State 1, $S2$ represents State 2 and so on.

$$m = \begin{bmatrix} 0 & \lambda_0 & 0 & 0 & 0 & 0 & 0 & 0 \\ 0 & 0 & \lambda_1 & 0 & 0 & 0 & 0 & 0 \\ 0 & 0 & 0 & \lambda_2 & 0 & 0 & 0 & 0 \\ 0 & 0 & 0 & 0 & \lambda_3 & 0 & 0 & 0 \\ 0 & 0 & 0 & 0 & 0 & \lambda_4 & 0 & 0 \\ 0 & 0 & 0 & 0 & 0 & 0 & \lambda_5 & 0 \\ 0 & 0 & 0 & 0 & 0 & 0 & 0 & \lambda_6 \\ 0 & 0 & 0 & 0 & 0 & 0 & 0 & 0 \end{bmatrix} \tag{2}$$

$$\lambda_0 S_0 = S_1 \tag{3}$$

$$\lambda_1 S_1 = S_2 \text{ and so on, till } \lambda_6 S_6 = S_7 \tag{4}$$

The second subdivision, which corresponds to EVs in charge and discharge mode, suggests that the batteries are discharged to power the vehicle and also that EVs are parked with an available charging slot that charges the battery. In this scenario, the battery can be discharged to any state and is charged from that particular state to any state. It is neither that battery is to be discharged to a depleted state only nor charged to the complete level only. In either case, any intermittent values are acceptable, and the model can be represented accordingly. Here, the model in Figure 8 represents 100% SOC to be the completely charged level and 30% SOC as the depleted state. The probability matrix 'n' of the battery discharge model is represented in (5), where μ represents the probability with which the battery is restored to its previous state.

$$n = \begin{bmatrix} 0 & \lambda_0 & 0 & 0 & 0 & 0 & 0 & 0 \\ \mu_0 & 0 & \lambda_1 & 0 & 0 & 0 & 0 & 0 \\ 0 & \mu_1 & 0 & \lambda_2 & 0 & 0 & 0 & 0 \\ 0 & 0 & \mu_2 & 0 & \lambda_3 & 0 & 0 & 0 \\ 0 & 0 & 0 & \mu_3 & 0 & \lambda_4 & 0 & 0 \\ 0 & 0 & 0 & 0 & \mu_4 & 0 & \lambda_5 & 0 \\ 0 & 0 & 0 & 0 & 0 & \mu_5 & 0 & \lambda_6 \\ 0 & 0 & 0 & 0 & 0 & 0 & \mu_6 & 0 \end{bmatrix} \tag{5}$$

It is clear that, in the last division, when the battery is in the charge period, the battery gets charged form the level it is discharged to. Considering that the battery is being charged from the empty state, i.e., State 7, the model can be represented as in Figure 9.

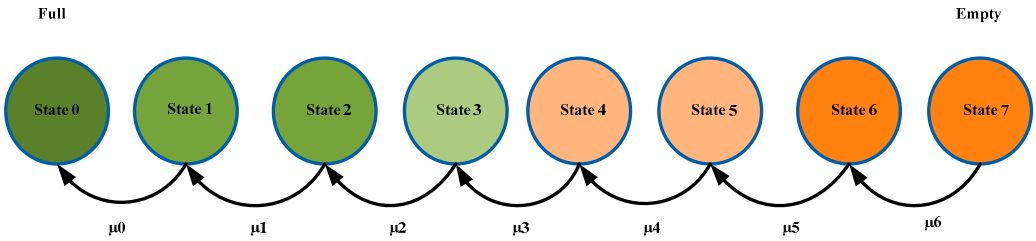

Figure 9. Battery charge model.

Considering the manufacturers' advice on the replacing of the batteries at the end of the specified duration, it can well be accounted that systematic replacement is a must for replacing worn-out battery immediately after a year. Likewise, an approximate life estimate of the batteries can be devised, as mentioned in Table 1, considering a whole sum replacement period of 8 years or 96 months. After 96 months, all the batteries are

replaced. Thus, in the specified the time interval of 96 months, an approximate life estimate of batteries is devised such that it adheres to the condition mentioned in (6).

$$\sum_{i=1}^{8} m_i = 100\% \tag{6}$$

Table 1. Battery replacement indicator.

Sl No.	Months	Percentage of Replacement (%)
1	12	1
2	24	3
3	36	5
4	48	10
5	60	15
6	72	20
7	84	26
8	96	20

If a battery is in the nth year, then it can either become 0 years old if replaced or can be a $(n + 1)$-year-old battery; this is a clear indication that the present age of the battery is dependent on its previous age. This scenario was accounted for, and a systematic model was developed by using Markov chain.

According to the Markov model, the initial computation matrix, $P(0)$, is represented in Equation (7). Transition probability matrix, m^n, for n step is represented in Equation (8). Using the theorem of total probability, we see that the consecutive transition of the states is given by Equation (9). The probability of the state of the system, p_j, after first transition can be represented by Equation (10).

$$P(0) = \begin{bmatrix} p_1(0) & p_2(0) & \dots & p_m(0) \end{bmatrix} \tag{7}$$

$$m^n = \frac{1}{m_{0.1} + m_{1.0}} \begin{bmatrix} m_{1.0} & m_{0.1} \\ m_{1.0} & m_{0.1} \end{bmatrix} + \frac{(1 - m_{0.1} - m_{1.0})^n}{m_{0.1} + m_{1.0}} \begin{bmatrix} m_{0.1} & -m_{0.1} \\ -m_{1.0} & m_{1.0} \end{bmatrix} \tag{8}$$

$$m(0) = \begin{bmatrix} \beta, & 1 - \beta \end{bmatrix} \tag{9}$$

$$p_j(1) = P(X_1 = j) = \sum_{1} P(X_1 = j)|X_0 = i)P(X_0 = i) \tag{10}$$

As the number of states considered is finite in number, the Markov chain is said to be ergodic, and the values of p_j must be unique.

4. Maintainability and Reliability Model of Electric Vehicle

The life cycle of a battery can contain a decreasing failure rate in early life, a sustained failure rate in its utility period and increasing failure rate during the end of its life cycle. The probability that a failure might not occur in the specified time interval is termed reliability [34]. There are several factors that contribute to the failure of a system. Indigent design and erroneous manufacturing techniques would contribute mainly to the failure, while incorrect operation methods, lack of system understanding and lack of skill set would add significantly to the failure of the system. Despite the best efforts, no system can be 100% reliable, and any system is bound to fail during its operation, which proves costly in terms of money, time and safety. This leads to substantial maintainability of the system, which becomes an essential consideration in regard to the long-term performance of the system. The system needs proper maintenance to avoid failures. Maintainability thus refers to restoring a faulty system back to its operational state in a specified time interval. The reliability and maintainability of the system forms the basis for the assessment of system availability which in turn integrates the system operation time, system fault identification time and its restoration time [35–37] Most of the analytical system considers only the failure

characteristics, while the repair process is considered to be negligible. However, it is an important metric to be considered to design the system. The Markov framework takes the edge off this and provides a substantial model. The basic framework is shown in Figure 10.

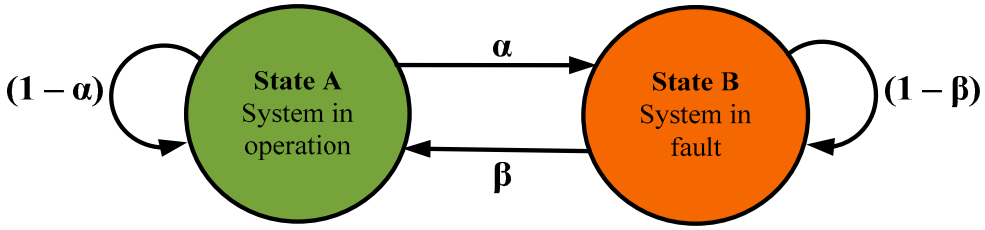

Figure 10. State space representation of system in operation and system in fault.

As shown in Figure 10, the parameter α represents the probability of change in the system from state of operation to fault state, and β represents the probability of change in the system from state of fault to state of operation, which can be represented as ratios mentioned in Equations (11) and (12). The fault rate and repair rate can be termed as mean operating time and mean down time. The transition probabilities from State A to State B for the system shown in Figure 10 can be represented in a probability transition matrix, as given in Equation (13).

$$\alpha = \frac{numberoffaultsinspecifiedtime}{durationofoperatingconditionofthesystem} \tag{11}$$

$$\beta = \frac{numberofrepairsinspecifiedtime}{durationofrepairmechanismofthesystem} \tag{12}$$

$$x = \begin{bmatrix} 1-\alpha & \alpha \\ \beta & 1-\beta \end{bmatrix} \tag{13}$$

For the system with continuous faults and repairs, the probability density function is always exponential. The reliability, r(t), and maintainability, m(t), of the system at any time, 't', is defined by Equations (14) and (15). For a system such as the electric vehicle (EV), as shown in Figure 11, the entire unit can be divided into two major units categorized as the Energy Unit (EU) and Propulsion Unit (PU). The EU comprises the Battery Unit (BU), Charge Control Unit (CCU) and Energy Management Unit (EMU), while the PU consists of the power converter (PC), propulsion motor (PM) and vehicle controller (VC). The reliability of the EV depends on the reliability of the EU and PU, as discussed in the sections below.

$$r(t) = e^{-\alpha t} \tag{14}$$

$$m(t) = 1 - e^{-\beta t} \tag{15}$$

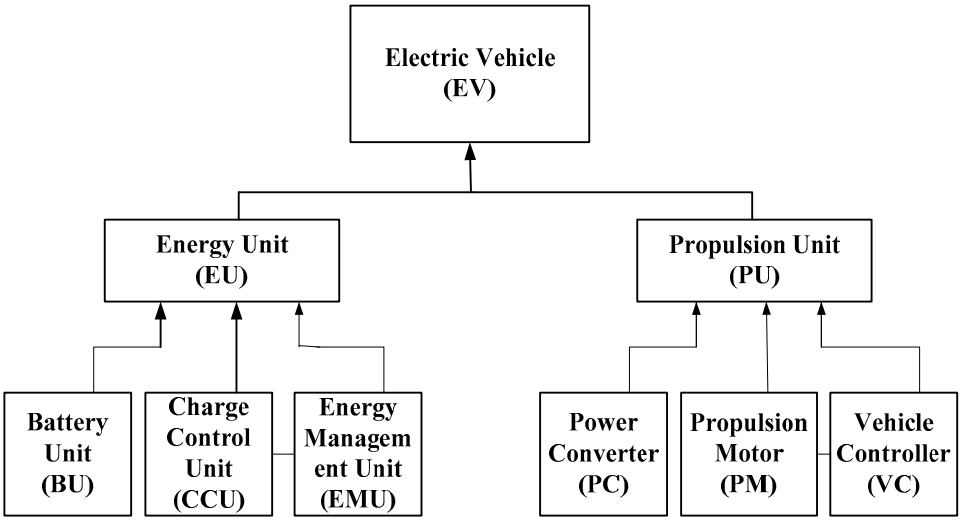

Figure 11. Electric-vehicle unit division.

4.1. Modeling and Analysis of Energy Unit (EU)

The reliability of the electric vehicle depends mainly on the Battery Unit (BU), which can be considered an essential part of the Energy Unit (EU) of the vehicle. At any given time, the BU may be in either the 'system in operation state' or 'system in fault state', which, in turn, represents the state of the electric vehicle. The faulty condition of the EU may occur due to two reasons. First, the battery might have lost all of its energy in powering up the vehicle—discharged state; and second, the battery would have lost its ability to store charge—broken state. Along with BU fault, the units such as the Charge Control Unit (CCU), which regulates the rate at which the battery is supplied with current for charging, and the Energy Management Unit (EMU), which prevents the battery from overcharging and undercharging, also play an important role in maintaining the operating condition of an electric vehicle. As discussed in the case of the BU, the CCU and EMU also have two states which can be in either the 'system in operation state' or 'system in fault state'. Therefore, the three different systems in two conditions result in a total of eight transitional combinations. Figure 12 shows the state space diagram of the EU, illustrating various transitions of different states. Moreover, α_{CCU}, α_{BU} and α_{EMU} represent the fault rates and β_{CCU}, β_{BU} and β_{EMU} represent the restoration rate of the CCC, BU and EU, respectively. The state space transition matrix (SSTM) of the EU is represented in Equation (16), where α_x, α_y, and α_z represent α_{CCU}, α_{BU} and α_{EMU}, respectively, and β_x, β_y, and β_z represent β_{CCU}, β_{BU} and β_{EMU}, respectively.

$$SSPM = \begin{bmatrix} 1-\alpha_x-\alpha_y-\alpha_z & \alpha_x & \alpha_y & \alpha_z & 0 & 0 & 0 & 0 \\ \beta_x & 1-\beta_x-\alpha_y-\alpha_z & 0 & 0 & \alpha_y & 0 & \alpha_z & 0 \\ \beta_y & 0 & 1-\alpha_x-\beta_y-\alpha_z & 0 & \alpha_x & \alpha_z & 0 & 0 \\ \beta_z & 0 & 0 & 1-\alpha_x-\alpha_y-\beta_z & 0 & \alpha_y & \alpha_x & 0 \\ 0 & \beta_y & \beta_x & 0 & 1-\beta_x-\beta_y-\alpha_z & 0 & 0 & \alpha_z \\ 0 & 0 & \beta_z & \beta_y & 0 & 1-\alpha_x-\beta_y-\beta_z & 0 & \alpha_x \\ 0 & \beta_z & 0 & \beta_x & 0 & 0 & 1-\beta_x-\alpha_y-\beta_z & \alpha_y \\ 0 & 0 & 0 & 0 & \beta_z & \beta_x & \beta_y & 1-\beta_x-\beta_y-\beta_z \end{bmatrix} \quad (16)$$

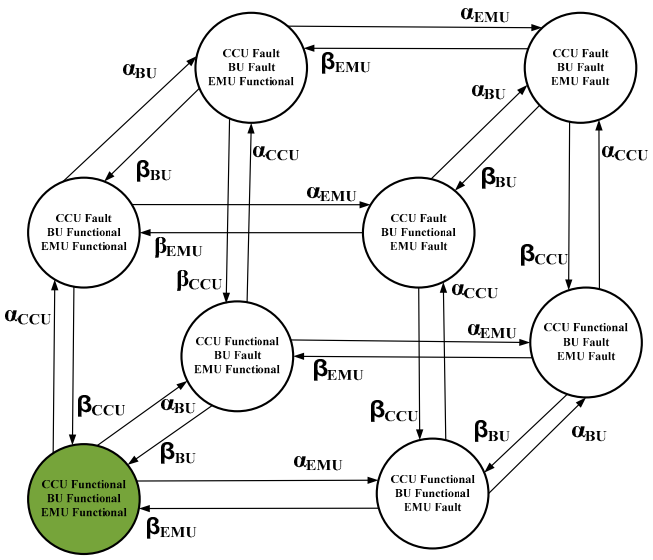

Figure 12. State space diagram of Energy Unit (EU).

The probability with which each state occurs in the model shown in Figure 12 can be found by using Equations (17)–(24).

$$P_{EU}^{(1)} = \frac{\beta_{CCU}\beta_{BU}\beta_{EMU}}{(\alpha_{CCU}+\beta_{CCU})(\alpha_{BU}+\beta_{BU})(\alpha_{EMU}+\beta_{EMU})} \tag{17}$$

$$P_{EU}^{(2)} = \frac{a_{CCU}b_{BU}b_{EMU}}{(a_{CCU}+b_{CCU})(a_{BU}+b_{BU})(a_{EMU}+b_{EMU})} \tag{18}$$

$$P_{EU}^{(3)} = \frac{\beta_{CCU}\alpha_{BU}\beta_{EMU}}{(\alpha_{CCU}+\beta_{CCU})(\alpha_{BU}+\beta_{BU})(\alpha_{EMU}+\beta_{EMU})} \tag{19}$$

$$P_{EU}^{(4)} = \frac{\beta_{CCU}\beta_{BU}\alpha_{EMU}}{(\alpha_{CCU}+\beta_{CCU})(\alpha_{BU}+\beta_{BU})(\alpha_{EMU}+\beta_{EMU})} \tag{20}$$

$$P_{EU}^{(5)} = \frac{\alpha_{CCU}\alpha_{BU}\beta_{EMU}}{(\alpha_{CCU}+\beta_{CCU})(\alpha_{BU}+\beta_{BU})(\alpha_{EMU}+\beta_{EMU})} \tag{21}$$

$$P_{EU}^{(6)} = \frac{\beta_{CCU}\alpha_{BU}\alpha_{EMU}}{(\alpha_{CCU}+\beta_{CCU})(\alpha_{BU}+\beta_{BU})(\alpha_{EMU}+\beta_{EMU})} \tag{22}$$

$$P_{EU}^{(7)} = \frac{\alpha_{CCU}\beta_{BU}\alpha_{EMU}}{(\alpha_{CCU}+\beta_{CCU})(\alpha_{BU}+\beta_{BU})(\alpha_{EMU}+\beta_{EMU})} \tag{23}$$

$$P_{EU}^{(8)} = \frac{\alpha_{CCU}\alpha_{BU}\alpha_{EMU}}{(\alpha_{CCU}+\beta_{CCU})(\alpha_{BU}+\beta_{BU})(\alpha_{EMU}+\beta_{EMU})} \tag{24}$$

The EU will be functional provided that all the other units are functional, that is, as represented by the equation $P_{EU}^{(1)}$, which is, in turn, representing the availability of the system. The remaining states, which represent at least one of the units in fault condition, makes the system to enter into fault state. Thus, the unavailability of the EU, U_{EU}, is the net probability of these seven states and can be calculated from Equation (25). After eliminating the fault states, the state space transition matrix reduces to the matrix $SSPM_Q$ given by Equation (26).

$$U_{EU} = \sum_{i=2}^{8} P_i \tag{25}$$

$$SSPM_Q = [1 - \alpha_{CCU} - \alpha_{BU} - \alpha_{EMU}] \tag{26}$$

The mean time that the EU is available in State 1 is determined by using Equation (27). The mean operating time of the EU, represented by EU_{MoT}, is given by Equation (28). The effective fault rate is, thus, given by Equations (29) and (30).

$$EU_M = \left[1 - SSPM_Q\right]^{-1} \tag{27}$$

$$EU_{MoT} = \frac{1}{\alpha_{CCU} + \alpha_{BU} + \alpha_{EMU}} \tag{28}$$

$$\alpha_{EU} = \frac{1}{EU_{MoT}} \tag{29}$$

$$\alpha_{EU} = \alpha_{CCU} + \alpha_{BU} + \alpha_{EMU} \tag{30}$$

The mean fault time, which is nothing but the mean time to restore the EU, is calculated by using Equation (31). The effective restoration rate of EU can be obtained by using Equations (32) and (33).

$$EU_R = \frac{1 - EU_A}{EU_A X \alpha_{EU}} \tag{31}$$

$$\beta_{EU} = \frac{1}{EU_R} \tag{32}$$

$$\beta_{EU} = \frac{EU_A X \alpha_{EU}}{1 - EU_A} \tag{33}$$

4.2. Modeling and Analysis of Propulsion Unit (PU)

The propulsion system mainly consists of a power converter (PC), propulsion motor (PM) and vehicle controller (VC). Each of these units can again be in either of two states, that is the 'system in operation state' or 'system in fault state'. The modeling and analysis of the Propulsion Unit is similar to that of the modeling and analysis of the Energy Unit of the electric vehicle shown in Figure 13. The availability of the PU is calculated by using Equation (34). The failure rate and restoration rates of the PU are also calculated in the same way as calculated for EU, given by Equations (35) and (36).

$$P_{PU} = \frac{\beta_{PC}\beta_{PM}\beta_{VC}}{(\alpha_{PC} + \beta_{PC})(\alpha_{PM} + \beta_{PM})(\alpha_{VC} + \beta_{VC})} \tag{34}$$

$$\alpha_{PU} = \alpha_{PC} + \alpha_{PM} + \alpha_{VC} \tag{35}$$

$$\beta_{PU} = \frac{P_{PU} X \alpha_{PU}}{1 - P_{PU}} \tag{36}$$

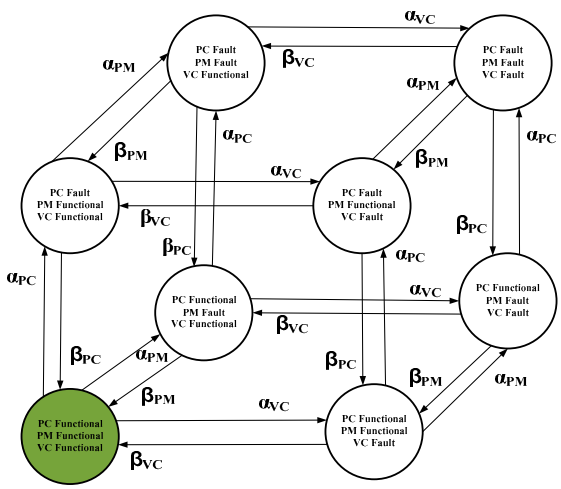

Figure 13. State space diagram of Propulsion Unit (PU).

4.3. Modeling and Analysis of EV System

As seen in the previous sections, for a successful operation of an EV, there must be successful operation of the two units of the EV, namely the EU and PU. The reliability model of the EV can be built as shown in Figure 14. EV system's functional states is directly dependent on functional states of EU and PU systems. The transition matrix of the EV is given in Equation (37). The availability of the EV is equal to the combined availability of the EU and PU, and this is determined by Equation (38).

$$SSPM_{EV} = \begin{bmatrix} 1-\alpha_{EU}-\alpha_{PU} & \alpha_{EU} & \alpha_{PU} & 0 \\ \beta_{EU} & 1-\beta_{EU}-\alpha_{PU} & 0 & \alpha_{PU} \\ \beta_{PU} & 0 & 1-\alpha_{EU}-\beta_{PU} & \alpha_{EU} \\ 0 & \beta_{PU} & \beta_{EU} & 1-\beta_{EU}-\beta_{PU} \end{bmatrix} \quad (37)$$

$$P_{EV} = \frac{\beta_{EU}\beta_{PU}}{(\alpha_{EU}+\beta_{EU})(\alpha_{PU}+\beta_{PU})} \quad (38)$$

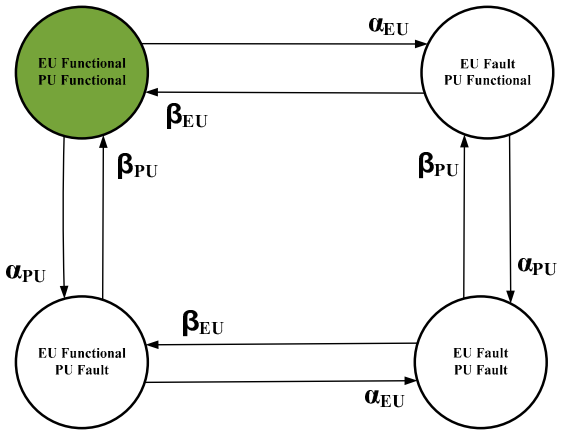

Figure 14. State space diagram of EV.

The availability of the EV can be found by using Equation (39), considering the available state only. Therefore, the mean time for first fault of an EV and the mean down time can be determined by using Equations (40) and (41):

$$SSPM_{QEV} = [1-\alpha_{EU}-\alpha_{PU}] \quad (39)$$

$$EV_{fault} = [1-SSPM_{QEV}]^{-1} \quad (40)$$

$$EV_{MDT} = \frac{1-P_{EV}}{P_{EV}X\alpha_{EV}} \quad (41)$$

Thus, the effective failure rate and repair rate of the EV are estimated by using Equations (42) and (43).

$$\alpha_{EV} = \frac{1}{EV_{fault}} = \alpha_{EU}+\alpha_{PU} \quad (42)$$

$$\beta_{EV} = \frac{1}{EV_{MDT}} = \frac{P_{EV}x\alpha_{EV}}{1-P_{EV}} \quad (43)$$

5. Analysis of Diesel-Renewable-Powered Electric Vehicle Charging System (EVCS)

In this section, an attempt is made to develop a grid-connected electric vehicle charging system to ensure surplus availability of the charging system to popularize the electric vehicle and, thus, enhance the sustainable transportation. The grid-connected EVCS can be considered as having an option of drawing/selling-back energy from/to the external grid. The model is represented in Figure 15. The capital cost the grid-integrated EVCS is

given in Table 2, and the sizing of the components and related information are provided in Table 3. The capital-cost and component-related information is obtained from the Hybrid Optimization of Multiple Energy Resources (HOMER) tool that has inbuilt algorithms to evaluate and assess the technical feasibility of integration of various energy resources.

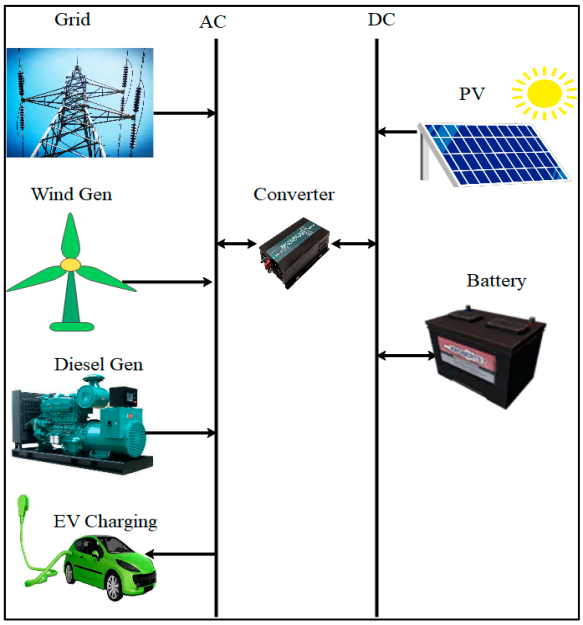

Figure 15. Diesel-renewable-based EVCS.

Table 2. Cost data of energy supply resources.

Component	Capital Cost ($)	Replacement Cost ($)	O&M Cost
PV	3000	2500	50 $/year
Wind	7000	7000	80 $/year
Diesel Generator	2250	2250	0.15 $/h
Battery	550	550	10 $/year
Converter	300	300	–

Table 3. Component sizing and other information.

Component	Options on Size and Unit Numbers	Life	Other Information
PV	10, 50, 100, 150, 200 kW	25 years	Derating Factor = 88%
Wind	10, 20, 30, 40, 50 Units	20 years	Hub Height = 24 m
Diesel Generator	10, 50, 100, 200, 500 kW	15,000 h	Minimum Load Ratio = 25%
Battery	50, 100,200,500 Units	15 years	Nominal Capacity = 167 Ah, 24 V
Converter	0, 10, 50, 100, 200, 500 kW	10 years	Converter Efficiency = 90% Rectifier Efficiency = 85%
Grid connection	10, 50,100, 500, 1000 kW	–	Purchase = 0.093 $/kWh Sellback = 0.036 $/kWh

6. Results and Discussion

6.1. R-C Model

The trust-region reflective nonlinear least-squares algorithm was employed, as the battery behavior is itself non-linear. The concept is to refine the parameters of interest with successive iterations. SOC vs. OCV for the 1 R-C to 5 R-C equivalent circuit model is shown in Figure 16. As the number of R-C branches increases, the accuracy increases. However, as assured that EVs are not allowed for deep discharge and longer full capacity run of EV,

limiting in the 20% to 85% of SOC, the 3 R-C equivalent model is sufficient to predict the behavior of the battery. The results are validated with the experimental data in accordance with standard drive cycles at different temperatures.

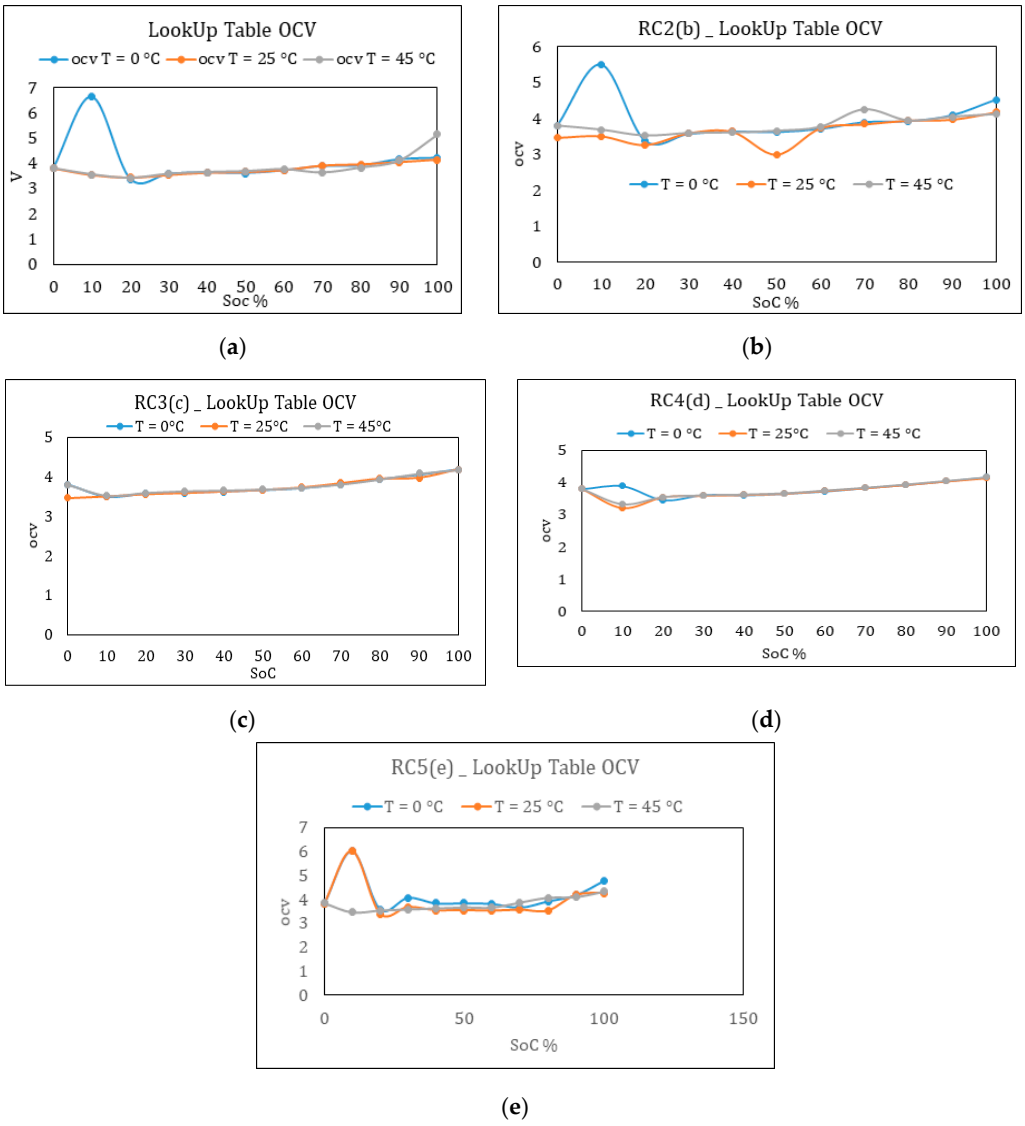

Figure 16. (**a**) OCV vs. SOC for 1 R-C, (**b**) OCV vs. SOC for 2 R-C, (**c**) OCV vs. SOC for 3 R-C, (**d**) OCV vs. SOC for 4 R-C and (**e**) OCV vs. SOC for 5 R-C.

6.2. Battery Ageing and Replacement

The proposed battery-replacement model results in the probability transition matrix represented in Equation (44) which states that if 1% of the battery is replaced, as given in Table 1, then the probability of replacement is 0.01, while the probability that it turns a year old is 0.99. If a battery is already a year old, then the probability that it would turn two years is 0.97, while having a probability of 0.03 for becoming 0 years on account of replacement of the battery.

$$p = \begin{bmatrix} 0.01 & 0.99 & 0 & 0 & 0 & 0 & 0 & 0 \\ 0.03 & 0 & 0.97 & 0 & 0 & 0 & 0 & 0 \\ 0.05 & 0 & 0 & 0.95 & 0 & 0 & 0 & 0 \\ 0.08 & 0 & 0 & 0 & 0.92 & 0 & 0 & 0 \\ 0.12 & 0 & 0 & 0 & 0 & 0.88 & 0 & 0 \\ 0.16 & 0 & 0 & 0 & 0 & 0 & 0.84 & 0 \\ 0.25 & 0 & 0 & 0 & 0 & 0 & 0 & 0.75 \\ 0.30 & 0 & 0 & 0 & 0 & 0 & 0 & 0 \end{bmatrix} \quad (44)$$

In accordance to electric vehicles, the steady-state probabilities are obtained by solving Equations (45) and (46). The solution for the entire set of linear equations is obtained as in Equation (47).

$$p_j(1) = P(X_1 = j) = \sum_1 P(X_1 = j)|X_0 = i)P(X_0 = i) \quad (45)$$

$$p_j(1) = \sum_1 p_i(0)p_{i,j} \quad (46)$$

$$\begin{bmatrix} {p_0}^* & {p_1}^* & {p_2}^* & {p_3}^* & {p_4}^* & {p_5}^* & {p_6}^* & {p_7}^* \end{bmatrix} = \begin{bmatrix} 0.1532 & 0.1599 & 0.1645 & 0.1673 & 0.1678 & 0.1671 & 0.1706 & 0.2072 \end{bmatrix} \quad (47)$$

The above calculation proclaims that 16% of batteries are one-year-old, and so on, and gives the critical piece of information that the battery will not be worn out within the stipulated ageing cycle, or the replacement period is small and is equal to 20%. It is evident that the whole-sum policy of replacing the battery only after specified calendar years is not reasonable, as many batteries are replaced in mid years of the specified time period. The average age of the batteries is computed to be 5 years. The transition-state diagram of battery-ageing model is given in Figure 17.

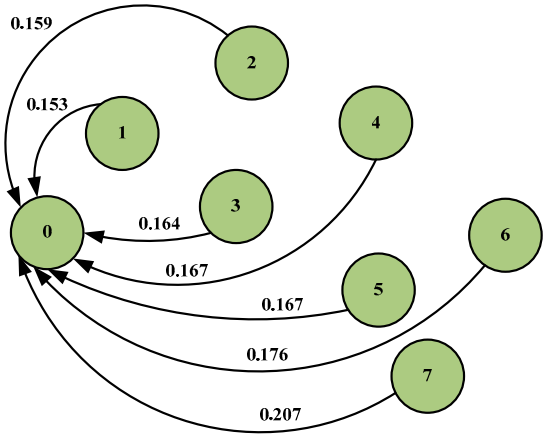

Figure 17. Transition diagram of battery ageing model.

6.3. EV Reliability and Maintainability

The reliability and maintainability of EV system at any time, '*t*', can be determined by using Equations (48) and (49):

$$R(t)_{EV} = 1 - e^{-\alpha_{EV}t} \quad (48)$$

$$M(t)_{EV} = 1 - e^{-\beta_{EV}t} \quad (49)$$

The analysis justifies that the reliability and availability of EVs degrade with time, due to various failures. However, with timely repair and replacement of faulty components, the vehicle's operational effectiveness can be improved significantly, as shown in Figure 18.

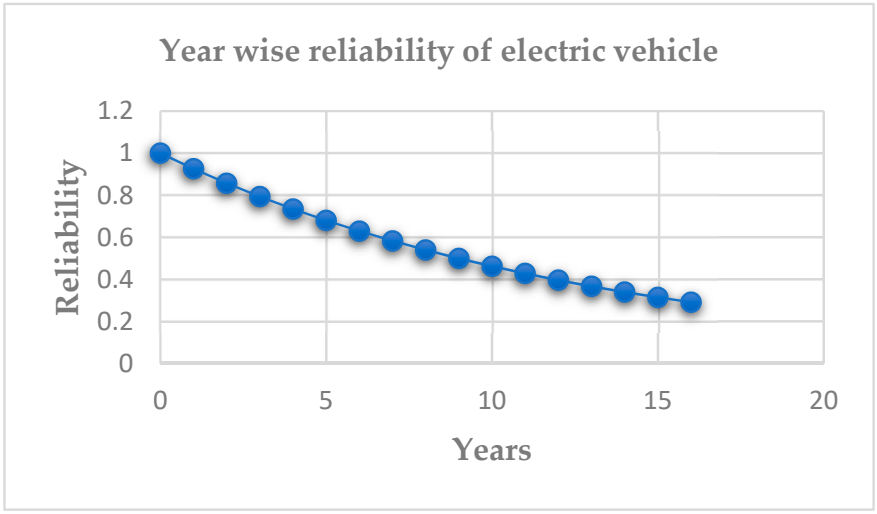

Figure 18. Year-wise reliability of electric vehicle.

6.4. Diesel-Renewable-Based EVCS

The monthly electricity production of diesel-based EVCS and the proposed diesel-renewable-based EVCS is shown in Figures 19 and 20, and the CO_2 emissions are shown in Figure 21. The main objective of this work was to reduce emissions by using green energy sources. By having multiple energy sources, the monthly electricity production also increases, and, at the same time, the electrical transaction with grid ensures the reduction in carbon emissions from 174,874 kg/year (diesel EVCS) to 76,525 kg/year (diesel-renewable-based EVCS).

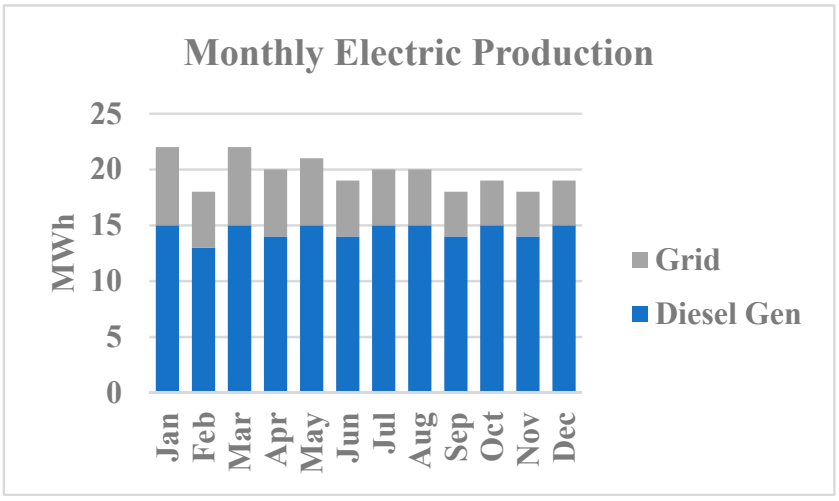

Figure 19. Monthly electricity production of diesel-based EVCS.

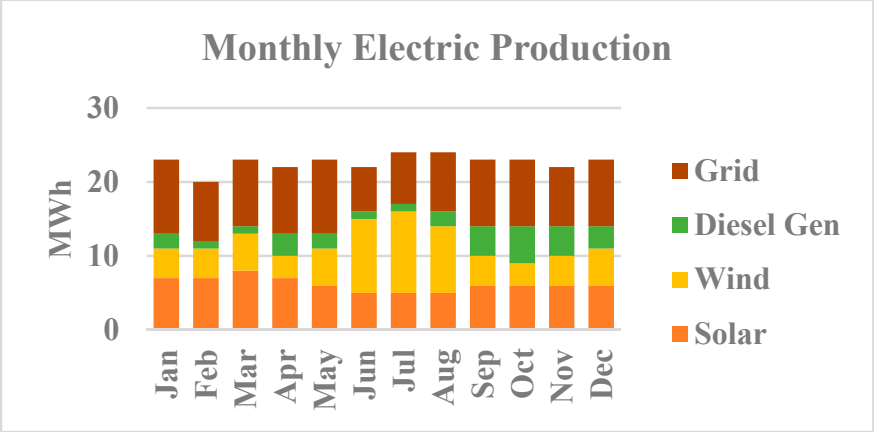

Figure 20. Monthly electricity production of diesel-renewable-based EVCS.

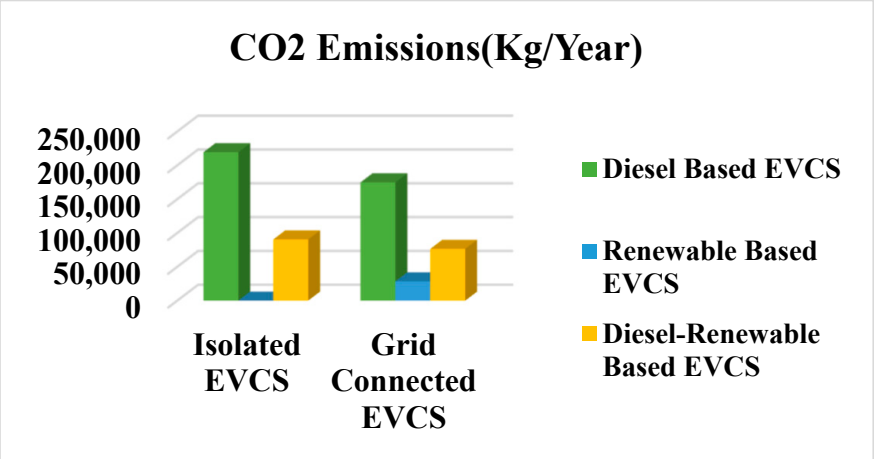

Figure 21. CO_2 emission of various EVCS.

7. Conclusions

In this paper, an ECM model was analyzed and experimentally validated, and it was found that the 3 R-C network is the best fit to represent the behavior of a battery. Stochastic models were developed for the battery ageing and replacement, using Markov chain, which provides a structured battery-replacement scheme. The significance of calendar ageing was also presented. A battery-powered electric vehicle was modeled, considering vital components of EV, and the reliability assessment was carried out to enhance the availability of EVs. Lastly, a case study of a diesel-renewable-based Electric Vehicle Charging Station (EVCS) in micro-grid was carried out. Technoeconomic and environment issues were presented, and it was found that the reliability on the grid purchase was reduced. The carbon emissions were reduced from 174,874 kg/year (diesel EVCS) to 76,525 kg/year (diesel renewable based EVCS).

Author Contributions: Conceptualization, S.B.S. and S.H.; Methodology, S.B.S. and S.H.; Resources, D.B. and B.B.; Writing—original draft, S.B.S.; Writing—review & editing, S.H. All authors have read and agreed to the published version of the manuscript.

Funding: This research received no external funding.

Institutional Review Board Statement: Not applicable.

Informed Consent Statement: Not applicable.

Data Availability Statement: Study did not report any data.

Acknowledgments: The authors are thankful to Centre for Advanced Life Cycle Engineering, University of Maryland, for making experimental test data public for academics and research.

Conflicts of Interest: The authors declare no conflict of interest.

Nomenclature

EV	electric vehicle
BMS	battery management system
ECM	Equivalent Circuit Model
EVCS	Electric Vehicle Charging Station
SOC	state of charge
OCV	Open Circuit Voltage
SEI	Solid Electrolyte Interface
α	probability of change in the system from state of operation to fault state
β	probability of change in the system from state of fault to state of operation
r(t)	reliability of the system
m(t)	maintainability of the system
EU	Energy Unit
PU	Propulsion Unit
BU	Battery Unit
CCU	Charge Control Unit
EMU	Energy Management Unit
PC	power converter
PM	propulsion motor
VC	vehicle controller
SSPM	state space transition matrix

References

1. Chaudhari, K.; Kandasamy, N.K.; Kanamarlapudi, R.K.; Gooi, H.B.; Ukil, A. Modeling of charging profiles for stationary battery systems using curve fitting approach. In Proceedings of the IECON 2017-43rd Annual Conference of the IEEE Industrial Electronics Society, Beijing, China, 29 October–1 November 2017; pp. 2777–2781.
2. El Ghossein, N.; Salameh, J.P.; Karami, N.; El Hassan, M.; Najjar, M.B. Survey on electrical modeling methods applied on different battery types. In Proceedings of the 2015 Third International Conference on Technological Advances in Electrical, Electronics and Computer Engineering (TAEECE), Beirut, Lebanon, 29 April–1 May 2015; pp. 39–44.
3. Timmermans, J.-M.; Nikolian, A.; De Hoog, J.; Gopalakrishnan, R.; Goutam, S.; Omar, N.; Coosemans, T.; Van Mierlo, J.; Warnecke, A.; Sauer, D.U.; et al. Batteries 2020—Lithium-ion battery first and second life ageing, validated battery models, lifetime modelling and ageing assessment of thermal parameters. In Proceedings of the 2016 18th European Conference on Power Electronics and Applications (EPE'16 ECCE Europe), Karlsruhe, Germany, 5–8 September 2016; pp. 1–23.
4. Muenzel, V.; de Hoog, J.; Brazil, M.; Vishwanath, A.; Kalyanaraman, S. A multi-factor battery cycle life prediction methodology for optimal battery management. In Proceedings of the 2015 ACM Sixth International Conference on Future Energy Systems, Bangalore, India, 14–17 July 2015; pp. 57–66.
5. Doyle, M.; Fuller, T.F.; Newman, J. Modeling of galvanostatic charge and discharge of the lithium/polymer/insertion cell. *J. Electrochem. Soc.* **1993**, *140*, 1526–1533. [CrossRef]
6. Fuller, T.F.; Doyle, M.; Newman, J. Simulation and optimization of the dual lithium ion insertion cell. *J. Electrochem. Soc.* **1994**, *141*, 1. [CrossRef]
7. Rakhmatov, D.; Vrudhula, S. An analytical high-level battery model for use in energy management of portable electronic systems. In Proceedings of the International Conference on Computer Aided Design (ICCAD'01), San Jose, CA, USA, 4–8 November 2001; pp. 488–493.
8. Chiasserini, C.; Rao, R. Pulsed battery discharge in communication devices. In Proceedings of the 5th International Conference on Mobile Computing and Networking, Seattle, WA, USA, 15–19 August 1999; pp. 88–95.
9. Chiasserini, C.; Rao, R. A model for battery pulsed discharge with recovery effect. In Proceedings of the Wireless Communications and Networking Conference, New Orleans, LA, USA, 21–24 September 1999; pp. 636–639.
10. Chiasserini, C.; Rao, R. Improving battery performance by using traffic shaping techniques. *IEEE J. Sel. Areas Commun.* **2001**, *19*, 1385–1394. [CrossRef]
11. Chiasserini, C.; Rao, R. Energy efficient battery management. *IEEE J. Sel. Areas Commun.* **2001**, *19*, 1235–1245. [CrossRef]
12. Tamilselvi, S.; Gunasundari, S.; Karuppiah, N.; Razak RK, A.; Madhusudan, S.; Nagarajan, V.M.; Sathish, T.; Shamim, M.Z.M.; Saleel, C.A.; Afzal, A. A Review on Battery Modelling Techniques. *Sustainability* **2021**, *13*, 10042. [CrossRef]
13. Ecker, M.; Gerschler, J.B.; Vogel, J.; Käbitz, S.; Hust, F.; Dechent, P.; Sauer, U. Development of a lifetime prediction model for lithium-ion batteries based on extended accelerated aging test data. *J. Power Sources* **2012**, *215*, 248–257. [CrossRef]

14. Grolleau, S.; Delaille, A.; Gualous, H.; Gyan, P.; Revel, R.; Bernard, J.; Redondo-Iglesias, E.; Peter, J. Calendar aging of commercial graphite/LiFePO4 cell–Predicting capacity fade under time dependent storage conditions. *J. Electrochem. Soc.* **2014**, *255*, 450–458. [CrossRef]
15. Naumann, M.; Schimpe, M.; Keil, P.; Hesse, H.C.; Jossen, A. Analysis and modeling of calendar aging of a commercial LiFePO4/graphite cell. *J. Energy Storage* **2018**, *17*, 153–169. [CrossRef]
16. Delaille, A.; Grolleau, S.; Ducland, F.; Bernard, J.; Revel, R.; Pelissier, S.; Iglesias, E.R.; Vinassa, J.M.; Eddahech, A.; Forgez, C.; et al. *SIMCAL Project: Calendar Ageing Results Obtained on a Panel of 6 Commercial Li-ion Cells*; ECS Meeting Abstracts, No. 14; The Electrochemical Society: San Francisco, CA, USA, 2013; p. 1191.
17. Ehsani, M.; Wang, F.-Y.; Brosch, G.L. (Eds.) *Transportation Technologies for Sustainability*; Springer: New York, NY, USA, 2013.
18. Chan, C.C.; Bouscayrol, A.; Chen, K. Electric, Hybrid, and Fuel-Cell Vehicles: Architectures and Modeling. *IEEE Trans. Veh. Technol.* **2010**, *59*, 589–598. [CrossRef]
19. Li, S.; Ke, B. Study of battery modeling using mathematical and circuit oriented approaches. In Proceedings of the 2011 IEEE Power and Energy Society General Meeting, Detroit, MI, USA, 24–28 July 2011; pp. 1–8.
20. Cao, Y.; Kroeze, R.C.; Krein, P.T. Multi-timescale parametric electrical battery model for use in dynamic electric vehicle simulations. *IEEE Trans. Transp. Electrif.* **2016**, *2*, 432–442. [CrossRef]
21. Obrovac, M.N.; Chevrier, V.L. Alloy negative electrodes for Li-ion batteries. *Chem. Rev.* **2014**, *114*, 11444–11502. [CrossRef] [PubMed]
22. Park, C.-M.; Kim, J.-H.; Kim, H.; Sohn, H.-J. Li-alloy based anode materials for Li secondary batteries. *Chem. Rev.* **2010**, *39*, 3115–3141. [CrossRef] [PubMed]
23. Delong, M.; Zhanyi, C.; Anming, H. Si-based anode materials for Li-ion batteries: A mini review. *Nano-Micro Lett.* **2014**, *6*, 347–358.
24. Czerepicki, A.; Koniak, M. *A Method of Computer Modeling the Lithium-Ion Batteries Aging Process Based on the Experimental Characteristics*; Warsaw University of Technology: Warszawa, Poland, 2017. [CrossRef]
25. Available online: https://www.edfenergy.com/electric-cars/batteries (accessed on 15 February 2022).
26. Available online: https://www.nissan.co.uk/ownership/nissan-car-warranties.html (accessed on 15 February 2022).
27. Available online: https://www.tesla.com/en_GB/support/vehicle-warranty?redirect=no (accessed on 15 February 2022).
28. Available online: https://www.chargedfuture.com/electric-car-battery-degradation (accessed on 15 February 2022).
29. Available online: https://www.greencarreports.com/news/1110881_how-much-is-a-replacement-chevy-bolt-ev-electric-car-battery (accessed on 15 February 2022).
30. Azkue, M.; Lucu, M.; Martinez-Laserna, E.; Aizpuru, I. Calendar Ageing Model for Li-Ion Batteries Using Transfer Learning Methods. *World Electr. Veh. J.* **2021**, *12*, 145. [CrossRef]
31. Barré, A.; Deguilhem, B.; Grolleau, S.; Gérard, M.; Suard, F.; Riu, D. A review on lithium-ion battery ageing mechanisms and estimations for automotive applications. *J. Power Sources* **2013**, *241*, 680–689. [CrossRef]
32. Redondo-Iglesias, E.; Venet, P.; Pelissier, S. Calendar and cycling ageing combination of batteries in electric vehicles. *Microelectron. Reliab.* **2018**, *88–90*, 1212–1215. [CrossRef]
33. Balagurusamy, E. *Reliability Engineering, First. P-24, Green Park Extension*; McGraw Hill Education (India) Private Limited: New Delhi, India, 2002.
34. Aggarwal, K.K. *Maintainability and Availability, Topics in Safety Reliability and Quality*; Springer: Dordrecht, The Netherlands, 1993; p. 16.
35. Shu, X.; Guo, Y.; Yang, W.; Wei, K.; Zhu, Y.; Zou, H. A Detailed Reliability Study of the Motor System in Pure Electric Vans by the Approach of Fault Tree Analysis. *IEEE Access* **2020**, *8*, 5295–5307. [CrossRef]
36. Billinton, R.; Allan, R.N. *Reliability Evaluation of Engineering Systems*; Springer: Boston, MA, USA, 1992.
37. Talukdar, B.K.; Deka, B.C. An Approach to Reliability, Availability and Maintainability Analysis of a Plug-In Electric Vehicle. *World Electr. Veh. J.* **2021**, *12*, 34. [CrossRef]